Characterization of titanium-containing catalysts by $^{47/49}$Ti solid-state NMR

Spectroscopic background: ^{47}Ti and ^{49}Ti nuclei have spins of I = 5/2 and 7/2, natural abundances of 7.44 % and 5.41 %, resonance frequencies of ν_0 = 28.195 and 28.203 MHz at B_0 = 11.75 T, and sensitivities of 1.6 x 10^{-4} and 2.0 x 10^{-4} in comparison with ^{1}H nuclei (1.0), respectively. These properties make ^{47}Ti and ^{49}Ti isotopes interesting candidates for solid-state NMR spectroscopy. Due to the quadrupole moments of Q = 30.2 x 10^{-30} m^2 for ^{47}Ti and Q = 24.7 x 10^{-30} m^2 for ^{49}Ti nuclei, their quadrupole coupling constants C_Q are large and similar at analogous structural sites. In the case of $^{47/49}$Ti solid-state NMR studies, the very small difference of the resonance frequencies of $\Delta\nu_0$ = 8 kHz at B_0 = 11.75 T leads often to an overlap of the spectral ranges of these two nuclei. For basic principles of solid-state NMR, see lectures “Solid-State NMR Spectroscopy” for Bachelor students or PhD seminars, accessible via the link “Lectures for Students”.

The most important titanium-containing materials are the **titanium oxide (TiO_2)** polymorphs anatase (metastable), brookite (metastable), and rutile (stable), which find broad applications in heterogeneous catalysis [1, 2] and photocatalysis [3, 4].

The tetragonal structure of **anatase** with the space group *I4*/*amd* has Ti sites with a 4-fold axis. By application of static $^{47/49}$Ti spin-echo NMR spectroscopy, these properties result in quadrupolar patterns with sharp singularities according to quadrupole coupling constants of $^{47Ti}C_Q$ = 5.85 MHz and $^{49Ti}C_Q$ = 4.79 MHz as well as an asymmetry parameter of $\eta_Q \cong 0$ (**Fig. 1a,** Fig. 1 in Ref. [5]). Considering the quadrupole moments Q of the ^{47}Ti and ^{49}Ti isotopes (*vide supra*), their quadrupole coupling constants are related by $^{49Ti}C_Q = 0.818 \cdot {}^{47Ti}C_Q$ or $^{47Ti}C_Q = 1.223 \cdot {}^{49Ti}C_Q$. Consequently, the experimental spectrum (bottom) is a superposition of a broad ^{47}Ti and a narrow ^{49}Ti quadrupolar pattern. For the anatase spectrum in **Fig. 1a**, solely the ^{49}Ti pattern was utilized for the simulation and determination of the C_Q and η_Q values. **Brookite** has an orthorhombic structure with the space group *Pbca.* The singularities of the quadrupolar patterns in the static $^{47/49}$Ti spin-echo NMR spectrum in **Fig. 1b** (Fig. 8 in Ref. [6]) correspond to $^{47Ti}C_Q$ = 7.3 MHz and $^{47Ti}C_Q$ = 5.97 MHz as well as an asymmetry parameter of η_Q = 0.55. For brookite, both the ^{47}Ti and the ^{49}Ti patterns were simulated, which clearly demonstrates their different frequency spread.

The structure of **rutile** has a space group *P4/mnm* and is body centred tetragonal. The quadrupolar pattern of rutile in **Fig. 1c** (Fig. 2 in Ref. [5]) has a considerably broader frequency spread than those of anatase and brookite, which is due to the space group *P4/mnm* with less symmetric local structures of the Ti sites. At the magnetic field of B_0 = 9.4 T, therefore, the experimentally observable quadrupolar pattern is mainly that of ^{49}Ti nuclei. Simulation of this pattern gives a quadrupole coupling constant of $^{49\text{Ti}}C_\text{Q}$ = 13.8 MHz and an asymmetry parameter of η_Q = 0.15. Approximately 500.000 scans with a repetition time of 0.1 s were collected for recording the static $^{47/49}$Ti spin-echo NMR spectrum of brookite at B_0 = 9.4 T within ca. 14 h [6].

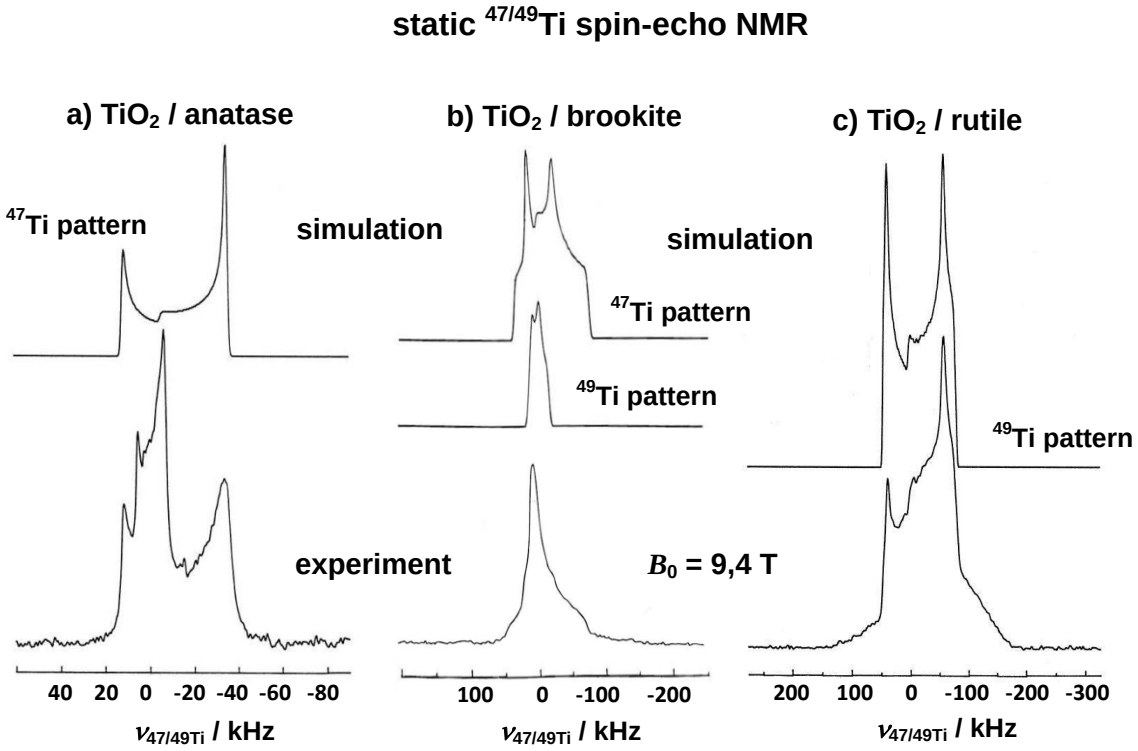

Fig. 1

The static $^{47/49}$Ti spin-echo NMR spectra in **Fig. 1** were recorded at a magnetic field of B_0 = 9.4 T and utilizing a solid-state NMR probe with a transverse coil for 10 mm sample tubes [5, 6]. Application of MAS NMR technique with a 9 mm rotor and sample spinning frequencies of ν_rot = 4 to 6 kHz at magnetic fields of B_0 = 11.7 T and 14.1 T is accompanied by a twice decrease of the frequency spread of the quadrupolar patterns (**Fig. 2**) [7]. MAS causes a decrease of the frequency spread of quadrupolar patterns by a factor of ca. 1/3.6 for equal B_0 values, while an increasing

magnetic field strength additionally decreases the frequency spread with $1/B_0$ (see page 24 of the lecture “Solid-State NMR Spectroscopy” for PhD seminars, accessible via the link “Lectures for Students”). Furthermore, the second-order quadrupole frequency shift ν_{qs} of the center of gravity ν_{cg} of the central transition in relation to the resonance position observed without quadrupolar interactions is decreased with $1/\nu_0$, i.e., $1/B_0$ (see page 12 in the above-mentioned lecture). For demonstration, **Fig. 2, left**, and **Fig. 2, right**, show $^{47/49}$Ti MAS NMR spectra of **anatase,** recorded at B_0 = 11.7 T and 14.1 T, respectively (Fig. 1 in Ref. [7]. Due to the smaller sample volume of the MAS rotors compared to the transverse 10 mm sample tubes utilized for the static spin-echo NMR studies in **Fig. 1**, the signal-to-noise ratio in **Fig. 2** is limited, especially for the ^{47}Ti patterns. On the other hand, the positions of the ^{47}Ti patterns are clearly separated from the ^{49}Ti patterns, as indicated by the simulated spectra (**bottom**).

For static $^{47/49}$Ti solid-state NMR and $^{47/49}$Ti solid-state NMR spectra of anatase and rutile recorded at B_0 = 28.2 T, see Supporting Information of Ref. [8].

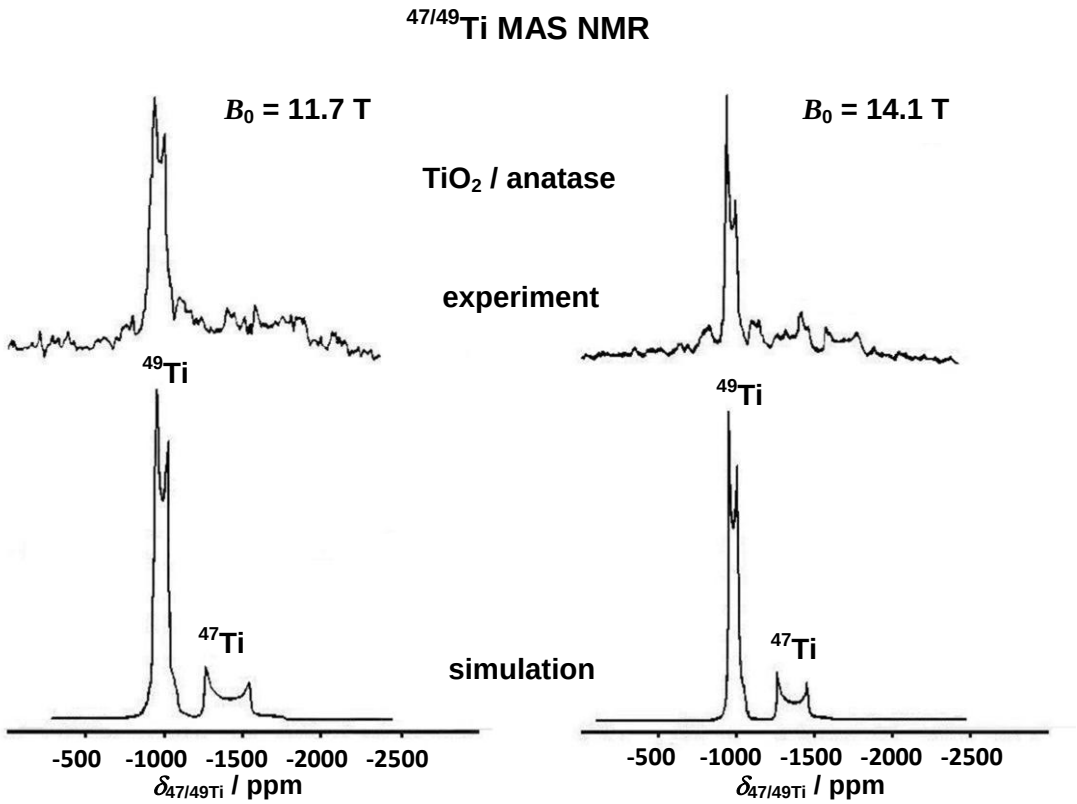

Fig. 2

In the field of heterogeneous catalysis, **TiO_2 is used as support material**, e.g. upon grafting with 10 wt% MoO_3 (MoO_3/TiO_2) [9]. One the other hand, also **supported**

titanium species, such as obtained by treatment of mesoporous silica nanoparticles (MSNs) with titanium isopropoxide followed by reaction with 1-methyl-3-[(triethoxysilyl)propyl]imidazolium chloride (IMILCl) and similar compounds, are in the focus of research [10, 11]. A very different approach is the preparation and study of **layered titanium phosphates (TiPs)** [12]. In all these cases, $^{47/49}$Ti solid-state NMR spectroscopy was utilized for gaining information on the nature of titanium species. The corresponding spectra were often recorded via application of the quadrupolar Carr-Purcell-Meiboom-Gill pulse group (QCPMG, see [13] and "method 15* as well as "method 17", accessible via the link "NMR Methods for Heterogeneous Catalysis") [9, 12] and, if possible, at high magnetic field (B_0 = 21.1 T [12]).

Numerous studies focused on **titanium-containing Ziegler-Natta catalysts**, which are important for the production of polyethylene and polypropylene in an industrial scale [14-17]. These catalysts consist of $MgCl_2$-supported $TiCl_4$ (**$TiCl_4/MgCl_2$**), prepared, e.g., by adsorption of liquid $TiCl_4$ on ball-milled $MgCl_2$, and sometimes additionally treated with BCl_3 [17]. The corresponding materials contain Ti species, which are diamagnetic and, therefore, accessible for $^{47/49}$Ti solid-state NMR spectroscopy. As an example, **Fig. 3, bottom**, shows the $^{47/49}$Ti QCPMG MAS NMR spectrum of the **Ziegler-Natta catalyst $TiCl_4/MgCl_2(THF1.5)\&BCl_3$**, recorded at B_0 = 21.1 T and with MAS at ν_{rot} = 10 kHz (Fig. 1 in Ref. [17]). With a recycle delay of

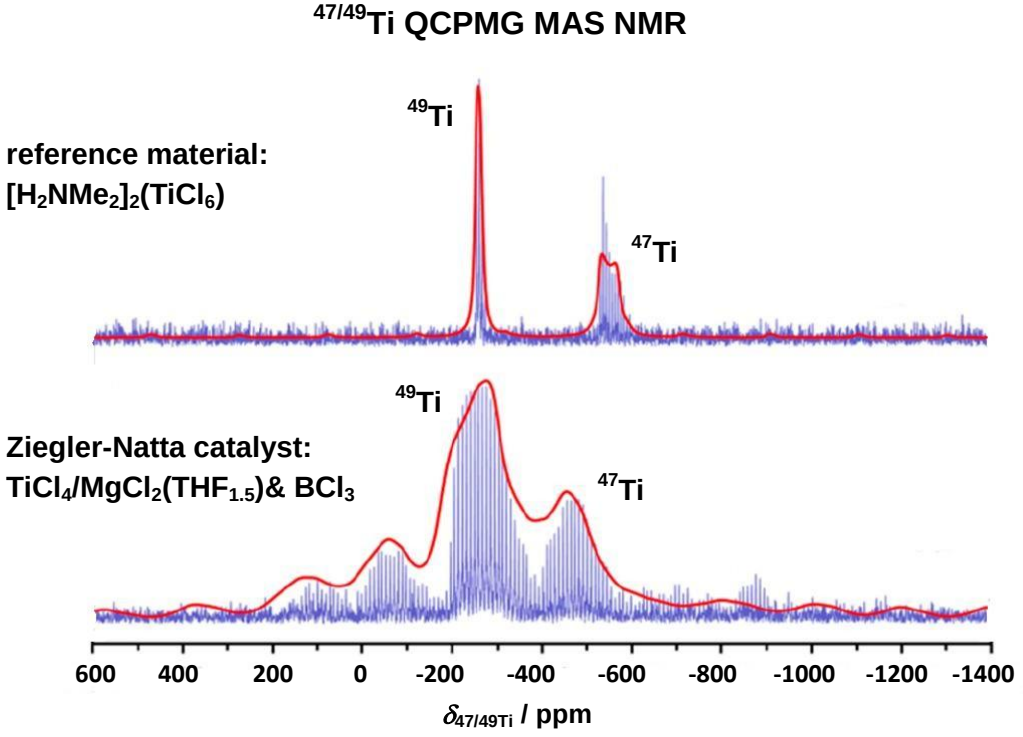

Fig. 3

1.5 s and 370.496 scans, recording the spectrum in **Fig. 3, bottom**, required 154.4 hours. As reference material, $[H_2NMe_2]_2(TiCl_6)$ was utilized (**Fig. 3, top**). The spectrum of $[H_2NMe_2]_2(TiCl_6)$ shows two relatively narrow signals (<1 kHz) corresponding to the ^{49}Ti and ^{47}Ti isotopes. Simulation of the spectrum yielded a quadrupole coupling constant of $^{49Ti}C_Q$ = 3.0 MHz and an isotropic chemical shift of δ_{iso} = −250 ppm. The $^{47/49}$Ti QCPMG NMR spectrum of the Ziegler-Natta catalyst $TiCl_4/MgCl_2$(THF1.5)&BCl_3 (**Fig. 3, bottom**) shows a much broader feature with numerous spinning sidebands, whose peak positions and widths are consistent with the surface Ti sites in a similar coordination environment as $[H_2NMe_2]_2[TiCl_6]$. The spectrum was simulated assuming identical Ti sites with a quadrupole coupling constant of $^{49Ti}C_Q$ = 9.3 MHz, an isotropic chemical shift of $^{49Ti}\delta_{iso}$ = −170 ppm, and an asymmetry parameter of η_Q = 0.65. This NMR signature is consistent with titanium atoms coordinated solely to Cl ligands in a distorted octahedral environment [17].

Titanium-containing materials with micro- and mesopore systems, such as **metal-organic frameworks (MOFs)** and zeolites are of high importance for shape-selective heterogeneous catalysis. Both the as-made and activated forms of the **MOF MIL-125(Ti)** were studied via static $^{47/49}$Ti solid-state NMR spectroscopy [18, 19], performed via coaddition of individual frequency-stepped subspectra, i.e. by a piecewise acquisition as variable-offset cumulative spectrum (VOCS, see Ref. [20] and “method 22”, accessible via the link “NMR Methods for Heterogeneous Catalysis”). At a magnetic field of B_0 = 21.1 T, this approach yielded a broad powder pattern ranging across ca. 200 kHz with a lake of any singularities or sharp edges. The quadrupolar pattern of the as-made MIL-125(Ti) exhibit some variance with values of $^{49Ti}C_Q$ = (16.4±1.2 MHz) and η_Q = (0.68±0.15). Upon activation, the width of the ^{49}Ti pattern decreased, corresponding to C_Q = (13.4±1.2) MHz and a drop in the asymmetry parameter to η_Q = (0.50±0.15) MHz. There was also a slight change in the isotropic chemical shift from δ_{iso} = -590 ppm for the as-made material to δ_{iso} = -658 ppm for the activated form [18, 19].

First $^{47/49}$Ti spin-echo NMR studies of the **titanosilicate TS-1** (MFI structure in **Fig. 4**, Scheme 1c in Ref. [8]) were performed at a magnetic field of B_0 = 7.0 T and delivered a broad (≅ 100 kHz) structure-less pattern, which was assigned to Ti species with a local structure to be close to an octahedrał coordination [21]. For more recent investigations of the titanosilicate TS-1, magnetic fields of B_0 = 18.8 T [22] and 28.2 T

MFI structure (left) and T-sites (right) of the titanosilicalite TS-1

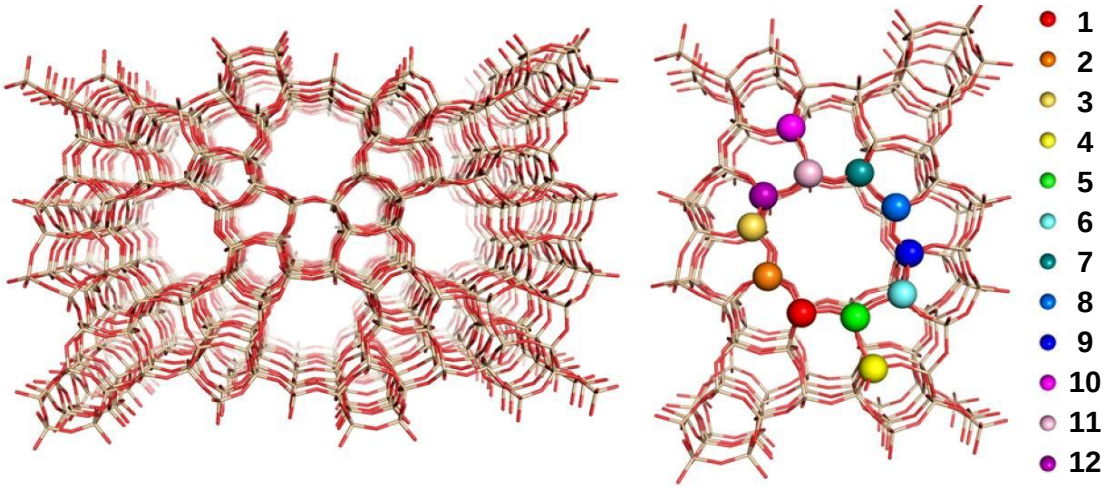

Fig. 4

[8] and the CPMG MAS technique with ν_{rot} = 15 kHz [22] and 20 kHz [8] were utilized. **Fig. 5** shows $^{47/49}$Ti QCPMG MAS NMR spectra of TS-1 materials with 1.0 wt% (a), 1.5 wt% (b), and 1.9 wt% (c) titanium atoms, recorded in the **dehydrated state (left)** and **upon hydration (right)**, the latter depicted in Supporting Information

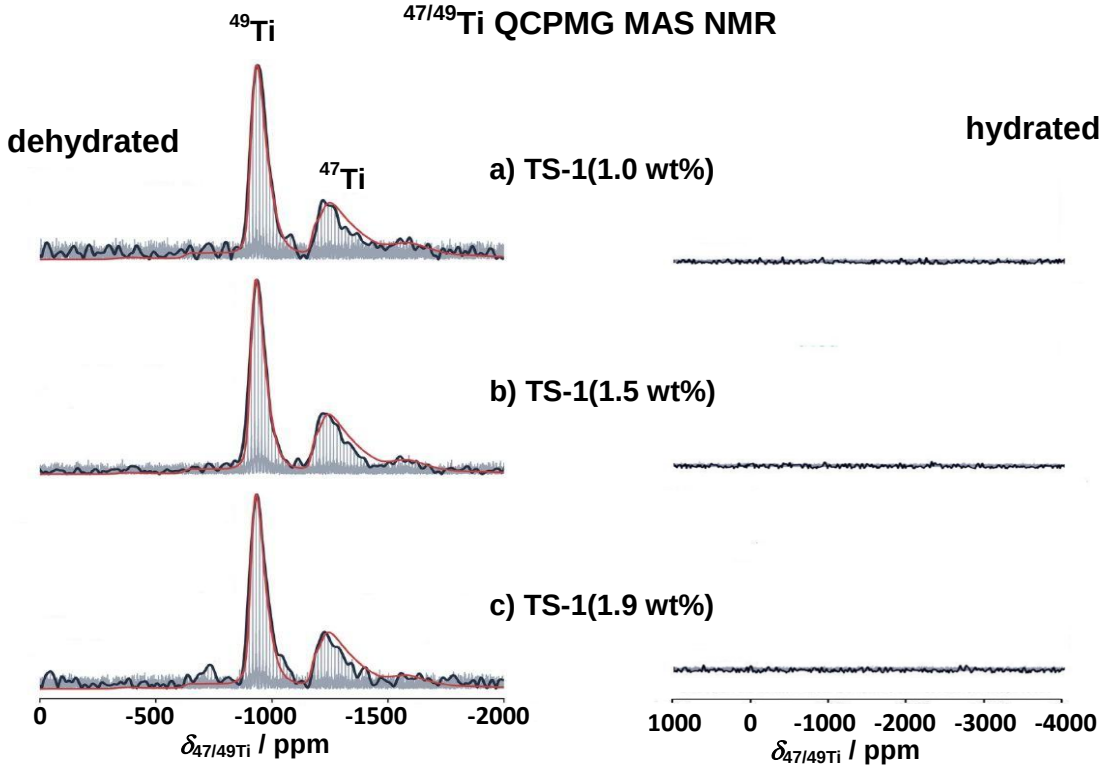

Fig. 5

of Ref. [8]. The spectra of the dehydrated TS-1 materials could be simulated by the same set of parameters, i.e., $^{49Ti}C_Q$ = 7.2 MHz, η_Q = 0.2, and δ_{iso} = -900 ppm, irrespective of the amount of Ti atoms incorporated into the framework. This observation indicates that the dominant Ti environment does not change upon incorporation of additional Ti atoms into the framework. This is consistent with similar catalyst performances, since all three zeolites showed high propylene epoxidation productivity [8]. Based on molecular model calculations, the $^{47/49}$Ti solid-state NMR parameters hint at the presence of isolated mononuclear Ti framework sites in the pristine TS-1 structure. Observed distributions of the NMR parameters presumably originate from variations of mononuclear Ti framework sites in the first and second coordination sphere and due to the occupancy of several T-sites (see **Fig. 3, right**) [8].

Interestingly, the $^{47/49}$Ti QCPMG MAS NMR signals visible in the spectra of the dehydrated TS-1 samples in **Fig. 5, left**, totally vanish upon hydration, as demonstrated by the spectra in **Fig. 5, right** [8]. This property was explained by the reaction of the Ti sites with water giving penta-coordinated species leading to quadrupole coupling constants, which are too large for detection by NMR at such low abundance, even at high magnetic fields [8]. On the other hand, the hydration-induced change of the $^{47/49}$Ti QCPMG MAS NMR signals of TS-1 is useful for the separation of signals of framework and extra-framework Ti species, occurring, e.g., in hierarchical titanosilicates. Generally, **hierarchical zeolites** combine primary micropores (less than 2 nanometers) with secondary mesopores (2 to 50 nanometers) or macropores (greater than 50 nanometers). The synthesis of **hierarchical TS-1** with 1.9 wt% titanium atoms (assigned TS-$1_{hierarchical}$(1.9 wt%)) enhances the exceptionally high activity of this titanosilicate by formation of extra-framework Ti species and mesopores, the latter by improving the reactant diffusion.

Fig. 6, top, (Fig. 4a in in Ref. [8]) shows $^{47/49}$Ti QCPMG NMR spectra of **dehydrated and hydrated TS-$1_{hierarchical}$(1.9 wt%)**. In contrast to the spectra of hydrated TS-1 samples, which were free of extra-framework Ti species in **Fig. 5, right**, the $^{47/49}$Ti QCPMG MAS NMR signals didn't totally vanish upon hydration of the hierarchical catalyst. This indicates that the latter catalyst contains extra-framework Ti species, which are not affected by hydration. Furthermore, the $^{47/49}$Ti QCPMG MAS NMR signatures of hydrated TS-$1_{hierarchical}$(1.9 wt%) and anatase nanoparticles show a

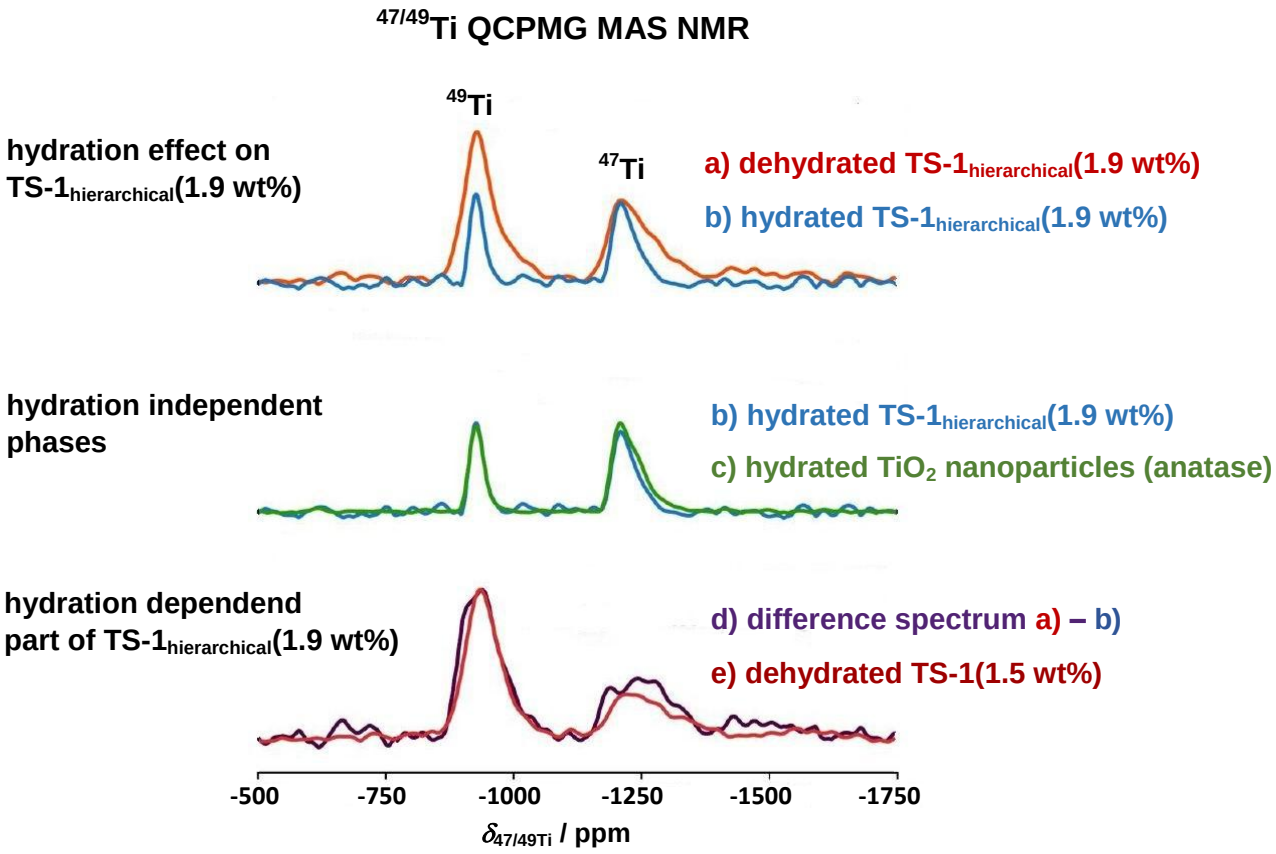

Fig. 6

significant resemblance (**Fig. 6, middle**). This indicates that the extra-framework Ti species are anatase-like phases rather than rutile-like phases, because the latter would exhibit significantly broader patterns (see **Fig. 1**). The difference spectrum of the hydrated and dehydrated TS-$1_{hierarchical}$(1.9 wt%), normalized by the number of scans, shows a strong resemblance with the $^{47/49}$Ti QCPMG MAS NMR signature of the dehydrated TS-1(1.5 wt%), which is free of extra-framework Ti species (**Fig. 6, bottom**). Hence, the $^{47/49}$Ti QCPMG MAS NMR spectrum of **dehydrated TS-$1_{hierarchical}$(1.9 wt%)** consists of two components, the signals of **framework Ti sites in TS-1(1.5 wt%)** and the signals of **extra-framework Ti species in anatase-like phases** [8].

In **Table** 1, a survey on $^{47/49}$Ti solid-state NMR parameters of Ti species in reference materials, solid catalysts, zeolite-like materials, and zeolites is given.

For a general overview on the recent state of solid-state NMR spectroscopy of low-γ nuclei, see Ref. [23].

Materials	$^{47Ti}C_Q$ / MHz *	$^{49Ti}C_Q$ / MHz *	η_Q	δ_{iso} / ppm	Refs.
TiO_2/anatase	5.85	4.79 [a]	0	-1.038 (-195 [b])	[5]
	5.9	4.85	0	-920	[24]
TiO_2/brookite	7.3	5.97 [a]	0.55	-943 (-100 [b])	[6]
TiO_2/rutile	16.9 [a]	13.8	0.15	-843 (0 [b])	[5]
Ti metal		9.25	0	Knight shift [c]	[5]
Ti_3Al		13.9	0.1	Knight shift [c]	[5]
TiAl		14.0	0	Knight shift [c]	[5]
$TiAl_2$		8.5	0.7	Knight shift [c]	[5]
$BaTiO_3$		3.78	0	-843 (0 [b])	[5]
solid $TiCl_2$	≅ 33	≅ 27	0		[16]
frozen $TiCl_4$	1.38	1.13	0.6	5	[16]
$TiCl_4/MgCl_2$		4.97	1	0 to -2.8	[14], [15]
$[H_2NMe_2]_2[TiCl_6]$		3.0		-250	[17]
Ziegler-Natta catalyst $TiCl_4/MgCl_2$(THF1.5)&BCl_3		9.3	0.65	-170	[17]
MOF MIL-125(Ti), as-made		16.4	0.68	-590	[18], [19]
MOF MIL-125(Ti), activated		13.4	0.5	-658	[18], [19]
Zeolite [Ti]USY	6.0	5.0	0.45	-850	[25]
Zeolite TS-1		7.2	0.2	-900	[8]

a) $^{49Ti}C_Q = 0.818 \cdot {}^{47Ti}C_Q$ or $^{47Ti}C_Q = 1.223 \cdot {}^{49Ti}C_Q$

b) referenced to powdered $SrTiO_3$ at δ_{iso} = 0 ppm [5], which has a shift of δ_{iso} = -843 ppm referenced to liquid $TiCl_4$ at δ_{iso} = 0 ppm [17, 26]

c) for Knight shift, see “method 22”

Sample preparation: The TiO_2 samples used for recording the $^{47/49}$Ti solid-state NMR spectra in **Figs. 1 and 2** were a commercial material (anatase, see Ref. [5]) or prepared as described for brookite in Ref. [6] and for rutile in Ref. [5]. These materials were investigated without any hydration or dehydration treatments.

For the $^{47/49}$Ti QCPMG MAS NMR spectrum of the Ziegler-Natta catalyst $TiCl_4/MgCl_2(THF1.5)\&BCl_3$ in **Fig. 3, bottom**, $TiCl_4$ was adsorbed on $MgCl_2$ followed by a BCl_3 treatment as described in detail in Ref. [27]. The reference material $[H_2NMe_2]_2(TiCl_6)$ used for recording the spectrum in **Fig. 3, top**, was prepared according to Ref. [28], but using DCM instead of $CHCl_3$ [17].

The TS-1 samples used for the $^{47/49}$Ti QCPMG MAS NMR studies shown in **Fig. 5** and **Fig. 6** were synthesized as described in the Supporting Information of Ref. [8]. The final calcination was performed at T = 763 to 773 K. Before the NMR studies, the samples were dehydrated for 10 h at T = 673 K under high vacuum, using a heating ramp of 200 K/h, and subsequently packed into MAS rotors inside an Ar-filled glovebox (< 0.5 ppm O_2, < 0.5 ppm H_2O) [8].

$^{47/47}$Ti solid-state NMR studies: The spectra in **Fig. 1** were recorded on a Bruker 400 MSL spectrometer operating at a magnetic field of B_0 = 9.4 T, a resonance frequency of ν_0 = 22.55 MHz, and using a probe with a transverse 10 mm coil. A two pulse echo sequence with 4 µs pulses, phase cycling, a pulse spacing range of τ = 150 to 350 µs, and recycle delays between 0.1 and 0.5 s were used [5].

The spectra in **Fig. 2** were recorded on Bruker AM-500 (B_0 = 11.7 T) and AM-600 (B_0 = 14.1 T) NMR spectrometers using home-built MAS probes. Torlon spinners with ~0.4 cm^3 sample volume and MAS speeds of ν_{rot} = 4 to 6 kHz were used. The spectra were obtained with a pulse sequence of the Hahn-echo type in order to eliminate artifacts due to transmitter and probe circuit “ringing" [7].

The spectra in **Fig. 3** were recorded on a Bruker 900 MHz (B_0 = 21.1 T) WB US2 NMR spectrometer equipped with a 3.2 mm triple-resonance MAS probe operating at $^{49Ti}\nu_0$ = 50.8 MHz. All measurements were conducted at $T \sim$ 100 K and at ν_{rot} = 10 kHz The samples were packed into 3.2 mm ZrO_2 rotors closed with Vespel drive caps with three layers of SharpieTM marker, to compensate for plastic contraction at $T \sim$ 100 K [17].

The spectra of the TS-1 samples in **Figs. 5 and 6** were acquired on a Bruker 1200 MHz NMR spectrometer at B_0 = 28.2 T corresponding to ν_0 = 67.6 MHz, equipped

with a 3.2 mm double-resonance MAS probe, and at ν_{rot} = 20 kHz. The dehydrated TS-1 samples were measured with SiO_2 plugs. For each spectrum, between 308.272 and 478.400 scans were acquired with a recycle delay of 0.25 s corresponding to measurement durations between 21.4 and 33.2 hours [8].

Generally, $^{47/49}$Ti solid-state NMR spectra are referenced to liquid **$TiCl_4$** at δ_{iso} = 0 ppm [7]. In Refs. [5] and [6], however, the spectra were referenced to powdered **$SrTiO_3$** at δ_{iso} = 0 ppm, which has a shift of $^{49Ti}\delta_{iso}$ = -843 ppm referenced to liquid **$TiCl_4$** at δ_{iso} = 0 ppm [26].

References:

[1] R.D. Hoval, S.T. Shinde, A.A. Kale, N.S. Gaikwad, G.S. Yedase, D.B. Bankar, K.G. Kanade, B. Dhokale, D.P. Amalnerkar, *TiO_2-based multifunctional catalytic systems for green and sustainable organic transformations: A comprehensive review*, RSC Adv. 16 (2026) 30538-30562, DOI: 10.1039/d6ra01453d.

[2] P. Eversfield, T. Lange, M. Hunger, E. Klemm, *Selective oxidation of o-xylene to phthalic anhydride on tungsten and tin promoted VO_x on TiO_2 monolayer catalysts*, Catal. Today 333 (2019) 120-126, DOI: 10.1016/j.cattod.2018.04.025.

[3] K. Nagaraj, S. Radha, C.G Deepa, K. Raja, V. Umapathy, N.P. Badgujar, N.M. Parekh, T. Manimegalai, L.A. Devi, C. Uthra, *Photocatalytic advancements and applications of titanium dioxide (TiO_2): Progress in biomedical, environmental, and energy sustainability*, Next Research 2 (2025) 100180, DOI: 10.1016/j.nexres.2025.100180.

[4] X. Sun, W. Dai, G. Wu, L. Li, N. Guan, M. Hunger, *Evidence of rutile-to-anatase photo-induced electron transfer in mixed-phase TiO_2 by solid-state NMR spectroscopy*, Chem. Commun. 51 (2015) 13779-13782, DOI: 10.1039/c5cc04971g.

[5] T.J. Bastow, M.A. Gibson, C.T. Forwood, *^{47,49}Ti NMR: Hyperfine interactions in oxides and metals*, Solid State Nucl. Magn. Reson. 12 (1998) 201-209, DOI: 10.1016/S0926-2040(98)00066-6.

[6] T.J. Bastow, G. Doran, H.J. Whitfield, Electron diffraction and ^{47,49}Ti and ^{17}O NMR studies of natural and synthetic brookite, Chem. Mater. 12 (2000) 436-439, DOI: 10.1021/cm990486m.

[7] S.F. Dec, M.F. Davis, G.E. Maciel, C.E. Bronnimann, J.J. Fitzgerald, S.-S. Han, *Solid-state multinuclear NMR studies of ferroelectric, piezoelectric, and*

related materials, Inorg. Chem. 32 (1993) 955-959, DOI: 10.1021/ic00058a034.

[8] C.J. Kaul, J. Koppe, L. Laetsch, M. Woerle, S. Aghazada, J.B. Holmes, C. Wartmann, M. Zheng, A. Berkessel, T. De Baerdemaeker, A.-N. Parvulescu, K. Seidel, J.H. Teles, A.V. Yakimov, C. Copéret, *Speciation, structural refinement, and distribution of Ti sites in titanium silicalite-1 from $^{47/49}$Ti NMR crystallography at 28.2 Tesla*, Angew. Chem. Int. Ed. 65 (2026) 65:e24232, DOI: 10.1002/anie.202524232.

[9] H. Nagashima, J. Trebosc, Y. Kon, K. Sato, O. Lafon, J.-P. Amoureux, *Observation of low-γ quadrupolar nuclei by surface-enhanced NMR spectroscopy*, J. Am. Chem. Soc. 142 (2020) 10659-10672, DOI: 10.1021/jacs.9b13838.

[10] P. Cruz, E.-A. Granados, M. Fajardo, I. del Hierroa, Y. Péreza, *Heterogeneous oxidative desulfurization catalysed by titanium grafted mesoporous silica nanoparticles containing tethered hydrophobic ionic liquid: A dual activation mechanism*, Appl. Catal. A, General 587 (2019) 117241, DOI: 10.1016/j.apcata.2019.117241.

[11] P. Cruz, Y. Perez, I. del Hierro, R. Fernandez-Gal, M. Fajardoa, *ε-Caprolactone polymerization using titanium complexes immobilized onto silica based materials functionalized with ionic liquids: insights into steric, electronic and support effects*, RSC Adv. 6 (2016) 19723-19733, DOI: 10.1039/c6ra01220e.

[12] J. Zhu, N. Trefiak, T.K. Woo, Y. Huang, *A $^{47/49}$Ti solid-state NMR study of layered titanium phosphates at ultrahigh magnetic field*, J. Phys. Chem. C 113 (2009) 10029-10037, DOI: 10.1021/jp901235w.

[13] I. Hung, Z. Gan, *On the practical aspects of recording wideline QCPMG NMR spectra*, J. Magn. Reson. 204 (2010) 256-265, DOI: 10.1016/j.jmr.2010.03.001.

[14] R. Ohashi, M. Saito, T. Fujita, T. Nakai, H. Utsumi, K. Deguchi, M. Tansho, T. Shimizu, *Observation of ^{47,49}Ti NMR spectra of $TiCl_4/MgCl_2$ catalysts under an ultrahigh magnetic field*, Chem. Lett. 41 (2012) 1563-1565, DOI: 10.1246/cl.2012.1563.

[15] T. Iijima, T. Shimizu, A. Goto, K. Deguchi, T. Nakai, R, ≅, M. Saito, *^{47,49}Ti solid-state NMR and DFT study of Ziegler-Natta catalyst: Adsorption of $TiCl_4$ molecule onto the surface of $MgCl_2$*, J. Phys. Chem. Solids 135 (2019) 109088, DOI: 10.1016/j.jpcs.2019.109088.

[16] E.S. (Merijn) Blaakmeer, F.J. Wensink, E.R.H. van Eck, G.A. de Wijs, A.P.M. Kentgens, *Preactive site in Ziegler-Natta catalysts*, J. Phys. Chem. C 123 (2019) 14490-14500, DOI: 10.1021/acs.jpcc.9b02617.

[17] A.V. Yakimov, C.J. Kaul, Y. Kakiuchi, S. Sabisch, F.M. Bolner, J. Raynaud, V. Monteil, P. Berruyer, C. Copéret, *Well-defined Ti surface sites in Ziegler−Natta pre-catalysts from $^{47/49}$Ti solid-state nuclear magnetic resonance spectroscopy*, J. Phys. Chem. Lett. 15 (2024) 3178-3184, DOI: 10.1021/acs.jpclett.3c03119.

[18] P. He, B.E.G. Lucier, V.V. Terskikh, Q. Shi, J. Dong, Y. Chu, A. Zheng, A. Sutrisno, Y. Huang, *Spies within metal-organic frameworks: Investigating metal centers using solid-state NMR*, J. Phys. Chem. C 118 (2014) 23728-23744, DOI: 10.1021/jp5063868.

[19] B.E. G. Lucier, S. Chen, Y. Huang, *Characterization of metal-organic frameworks: Unlocking the potential of solid-state NMR*, Acc. Chem. Res. 51 (2018) 319-330, DOI: 10.1021/acs.accounts.7b00357.

[20] G.J. Rees, S.T. Orr, L.O. Barrett, J.M. Fisher, J. Houghton, G.H. Spikes, B.R.C. Theobald, D. Thompsett, M.E. Smith, J.V. Hanna, *Characterisation of platinum-based fuel cell catalyst materials using ^{195}Pt wideline solid state NMR*, Phys. Chem. Chem. Phys. 15 (2013) 17195-17207, DOI: 10.1039/c3cp52268g.

[21] A. Lopez, M.H. Tuilier, J.L. Guth, L. Delmotte, J. M. Popa, *Titanium in MFI-type zeolites: A characterization by XANES, EXAFS, IR, and ^{74,49}Ti and ^{17}O MAS NMR spectroscopy and H_2O adsorption*, J. Solid State Chem. 102 (1993) 480-491, DOI: 10.1006/jssc.1993.1060.

[22] L. Laetsch, C.J. Kaul, A.V. Yakimov, I.B. Mueller, A. Hassan, B. Perrone, S. Aghazada, Z.J. Berkson, T. De Baerdemaeker, A.-N. Parvulescu, K. Seidel, J.H. Teles, C. Copéret, *NMR signatures and electronic structure of Ti sites in titanosilicalite-1 from solid-state $^{47/49}$Ti NMR spectroscopy*, J. Am. Chem. Soc. 145 (2023) 15018-15023, DOI: 10.1021/jacs.2c09867.

[23] M.E. Smith, *Recent progress in solid-state nuclear magnetic resonance of half-integer spin low-γ quadrupolar nuclei applied to inorganic materials*, Magn. Reson. Chem. 59 (2021) 864-907, DOI: 10.1002/mrc.5116.

[24] L.V. Dmitrieva, L.S. Vorotilova, I.S. Podkorytov, M E. Shelyapina, *A comparison of NMR spectral parameters of ^{47}Ti and ^{49}Ti nuclei in rutile and anatase*, Phys. Solid State 41 (1999) 1097-1099, DOI: 10.1134/1.1130944.

[25] S. Ganapathy, K. U. Gore, R. Kumar, J.-P. Amoureux, *Multinuclear (^{27}Al, ^{29}Si, ^{47,49}Ti) solid-state NMR of titanium substituted zeolite USY*, Solid State Nucl. Magn. Reson. 24 (2003) 184-195, DOI: 10.1016/S0926-2040(03)00044-4.

[26] A.J. Rossini, I. Hung, R.W. Schurko, *Solid-State $^{47/49}$Ti NMR of titanocene chlorides*, J. Phys. Chem. Lett. 1 (2010) 2989-2998, DOI: 10.1021/jz1012017.

[27] M. Humbert, S. Norsic, J. Raynaud, V. Monteil, *Activity enhancement of $MgCl_2$-supported Ziegler-Natta catalysts by Lewis acid pre-treatment for ethylene polymerization*, Chin. J. Polym. Sci. 37 (2019) 1031-1038, DOI: 10.1007/s10118-019-2335-8.

[28] S. Rannabauer, W. Schnick, Synthese, *Kristallstruktur und spektroskopische Charakterisierung von Bis-(dimethylammonium)hexachlorotitanat $[Me_2NH_2]_2[TiCl_6]$*, Z. Naturforsch. B 58 (2003) 410-414, DOI: 10.1515/znb-2003-0509.